communications earth & environment

Article

A Nature Portfolio journal

https://doi.org/10.1038/s43247-025-02525-5

Natural variability-focused assessment of climate overshoot timing

Josef Ludescher [1] ✉, Naiming Yuan [2,3,4] ✉, Hans Joachim Schellnhuber[5,6] & Armin Bunde[7]

The Paris Agreement legally commits the international community to keep anthropogenic global warming well below 2.0 °C, while efforts shall be made to hold the 1.5 °C-line. Under climate business as usual, however, the transgression of those lines will happen in the next few decades, causing major adaptation challenges. Fully-fledged Earth System Models are usually employed for concrete overshoot-timing projections, yet they are not only computationally expensive, but their internal variability is model dependent, which may significantly distort (and invalidate) their projections. Here we present, as an alternative, a purely data-driven approach based on the persistence properties of the observed global temperatures. We quantify, in a probabilistic way, the natural variability that must be superimposed on the anthropogenic trends in order to retrieve the observed warming behavior. When assuming that the anthropogenic warming continues at the current rate, we actually arrive at comparable overshoot timing estimates as the Earth System Models and provide an explanation for this finding. Since the two approaches are independent, they support each other strongly and highlight the need for an effective overshoot management.

Ever since the Paris Agreement in 2015, "holding the increase in the global average temperature to well below 2.0 °C above pre-industrial levels and pursuing efforts to limit the temperature increase to 1.5 °C above pre-industrial levels" has become an international goal that requires efforts of humanity. In spite of recent activities on limiting carbon emissions[1], however, we are still on the track of approaching the 1.5 °C threshold[2]. In 2018, the Intergovernmental Panel on Climate Change (IPCC) Special Report on 1.5 °C indicated that the 1.5 °C warming level is likely to be exceeded (with 66% probability) between 2030 and 2052 if global warming "continues to increase at the current rate"[3]. More recently, the IPCC AR6[4] reported that in all scenarios considered in WGI except the very high emissions scenario (SSP5-8.5), the midpoint of the first 20-year running average period during which the assessed global average temperature change reaches 1.5 °C lies in the first half of the 2030s. Only in the very high greenhouse gas emissions scenario is the midpoint in the late 2020s. On the other hand, the running 12-months mean for the global surface temperature has recently transgressed the 1.5 °C-line already[5], but this may be just a short overshoot episode.

In their projections, the IPCC considered a 20-year average for the warming level (see also the Discussion in refs. 6,7). The 20-year average may, to some extent, filter out the natural cycles, but this may not be sufficient in view of the multiple-scale variability of the climate system[8]. In addition, the recently discussed "hot model" problem in many ESMs may enhance the uncertainties of the ESM's projections[9,10]. Different approaches have been suggested to arrive at a best aggregated estimate based on the ESM's outputs, in particular, to reconcile them with historical observations[11–13].

In general, the global average temperature is composed of an anthropogenic warming trend and a stochastic natural trend. The anthropogenic trend is the response to the anthropogenic forcings[4], which include forcings due to greenhouse gases, aerosols and land use changes, and is relevant for the Paris Agreement. We would like to note that in this study, we consider the *effective* anthropogenic trend, which results from all the anthropogenic forcings. The natural trend arises from the natural variability and includes the response to forcings like the solar cycle and volcanism. The natural trends are superimposed on the anthropogenic trend and may either enhance or decrease it, as, for example, in the rapid warming period from the late 1970s to the late 1990s or in the "global warming hiatus" period afterwards[14,15].

Accordingly, a proper consideration of the natural variability in the global mean temperature series is essential for the estimation of the magnitude of present and future anthropogenic trends. For instance, imagine in a "gedankenexperiment" that the natural fluctuation of the global mean temperature was extremely large, say, of the order of 3 °C per decade. In such a scenario, it cannot be ruled out that a stochastic non-anthropogenic warming

[1]Potsdam Institute for Climate Impact Research (PIK), Member of the Leibniz Association, 14412 Potsdam, Germany. [2]School of Atmospheric Sciences, Sun Yat-sen University, Zhuhai, China. [3]Key Laboratory of Tropical Atmosphere-Ocean System, Ministry of Education, Zhuhai, China. [4]Southern Marine Science and Engineering Guangdong Laboratory, Zhuhai, China. [5]International Institute for Applied Systems Analysis (IIASA), 2361 Laxenburg, Austria. [6]Department of Earth System Science, Tsinghua University, Beijing, China. [7]Institute for Theoretical Physics, Justus Liebig University Giessen, 35392 Giessen, Germany.
✉e-mail: josef.ludescher@pik-potsdam.de; yuannm@mail.sysu.edu.cn

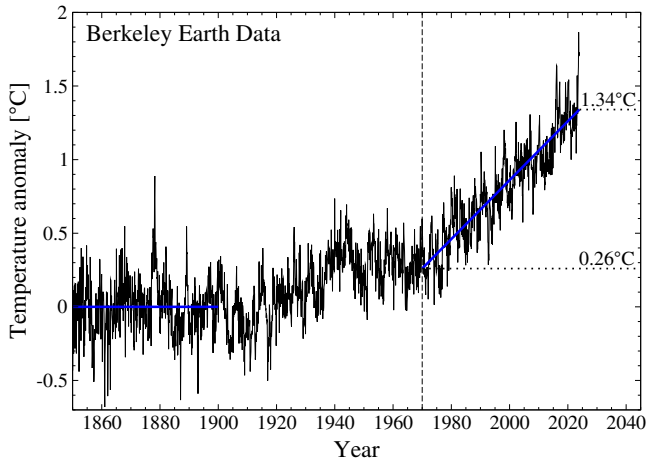

Fig. 1 | Global mean surface temperature (GMST) of the Berkeley Earth data set. The figure shows the deviation of the GMST from the pre-industrial period 1850–1900 (blue horizontal line). In the (approximately) linear trend regime between January 1970 and December 2023, we performed a linear regression analysis. At the endpoints of the (blue) regression line, the temperature difference is 0.26 °C and 1.34 °C. The standard deviation of the data around the trend line is $\sigma = 0.149$ °C. The HadCRUT data show a similar development, with slightly lower endpoints of the regression line (0.20 °C and 1.27 °C), and $\sigma = 0.140$ °C.

excursion pushes the global temperature above 2.0 °C in the medium term. In contrast, a strong negative natural trend could delay the breaching of the 2.0 °C-guardrail by several decades. In such an extreme scenario, the steady anthropogenic trend would dominate in the very long run only.

Here we develop a data-driven stochastic approach to address the above challenges, which is based solely on observational data and is thus complementary to the ESMs. ESMs consider natural trends by directly simulating the components of the Earth system and their interactions. Based on the ESM approach, single-model initial-condition large ensembles (SMILEs) (e.g., ref. 16), provide a way to obtain estimates of the internal variability by running an individual ESM many times with different initial conditions. Calculating the ensemble statistics around the mean forced response allows then to estimate the internal variability within the model. However, such a SMILE does not represent an unbiased sample from the underlying probability distribution. Indeed, the model-to-model differences in temperature projections can be larger than the internal variability within a SMILE (e.g., refs. 17,18). Additionally, even the initialization procedure of the same ESM can influence the model's internal variability[19]. To mitigate modeling errors and to obtain more reliable projections, the outputs of different ESMs can be combined, but the results depend on the applied weighting scheme[20]. Thus, the uncertainty in ESM-based projections, given a shared socioeconomic pathway (SSP) forcing scenario, depends markedly on the inter-model uncertainty and how to handle it best, while their simulated internal variability represents only a part of the uncertainty. In contrast, our approach explicitly considers the role of the natural trends. It exploits the fact that the natural trends in an observed record are closely related to its persistence properties: records with strong serial autocorrelations show a pronounced "mountain-valley" structure[21,22], which reflects the presence of natural trends[23–26]. It is well known that the global average temperature is characterized by strong long-term correlations with a Hurst exponent[21,27] close to 1 (e.g., ref. 28 and references therein).

Using this feature, we can generate surrogate data that reflect the natural variability of the global average temperature and obtain the probability distribution of the expected natural trends. Under the assumption that the anthropogenic warming trend continues to increase at the present rate, this allows us to estimate, in a straightforward probabilistic way and independently of the computationally demanding ESM simulations, the likely and very likely time span when the 1.5 °C and 2.0 °C thresholds will be lastingly exceeded. The method allows also to estimate efficiently the likely and very likely temperature ranges in the near-term, around 2031, and in the mid-term, around 2051. The uncertainty in the current natural trend leads to an uncertainty in the magnitude of the current anthropogenic trend. This uncertainty extends into the future and directly determines the uncertainty in the quantities considered here.

Results

Anthropogenic warming rate of the past 54 years

We consider the Berkeley Earth and HadCRUT temperature datasets, which represent the global mean surface temperatures (GMST)[29,30] between 1850 and 2023 and are widely used in climate science (see "Methods"). Figure 1 shows the Berkeley Earth data. Between 1850 and 1900, the data fluctuate around a constant temperature value, which we set to zero here. Between 1920 and 1940, the temperature increases by about 0.26 °C and fluctuates around this value for the next 30 years. After January 1970, the temperature increases approximately linearly and fluctuates around the trend line. For analyzing this trend, which is most relevant for estimating the future development, we perform a linear regression analysis. A linear regression is sufficient since assuming a quadratic trend would improve the explained variance only marginally, and the additional fit parameter is not justified by the data, see Supplementary Note 1. We find that the temperature difference Δ_{off} between the pre-industrial period 1850–1900 and the start point of the regression line in January 1970 is 0.26 °C in the Berkeley Earth record. In the linear trend regime between 1970 and 2023, the temperature increase is $\Delta^* = 1.08$ °C and the standard deviation σ around the trend line is 0.149 °C. For the HadCRUT record, $\Delta_{\text{off}} = 0.20$ °C, $\Delta^* = 1.07$ °C and $\sigma = 0.140$ °C.

In the following, we focus on the linear temperature regime. We are interested in the anthropogenic part Δ_A of the warming trend. Since the anthropogenic trend Δ_A and the natural trend Δ contained in Δ^* are superimposed, we have

$$\Delta_A = \Delta^* - \Delta. \tag{1}$$

Accordingly, depending on the sign of Δ, the anthropogenic trend Δ_A can be larger or smaller than the measured trend Δ^*.

To quantify the uncertainty in the anthropogenic trend, we consider the q-quantile Δ_q, which is related to the probability density $P(\Delta)$ of the natural trends by

$$\int_{\Delta_q}^{\infty} d\Delta P(\Delta) = q, \;\; 0 \le q \le 1, \;\; -\infty < \Delta_q < \infty. \tag{2}$$

By definition, natural trends above Δ_q occur with probability q. Since positive and negative natural trends are equally likely, $\Delta_{0.5} = 0$ and $\Delta_{1-q} = -\Delta_q$. Accordingly, the anthropogenic trend is with probability q above $\Delta^* + \Delta_q$ or below $\Delta^* - \Delta_q$. As a consequence, the observed temperature increase Δ^* is the median estimate of the anthropogenic trend, see also Supplementary Note 2.

To obtain Δ_q, we use the fact that the global average temperature data are long-term persistent with Hurst exponents close to 1[28]. This feature allows to generate a large number of surrogate data with the same natural variability as the two GMST records, and to determine the desired q-quantiles. The procedure is described in the "Methods" section and consists of 3 steps; we describe them here for the Berkeley record.

(i) First, to evaluate the long-term persistence of the record, we apply the detrended fluctuation analysis of order 3 (DFA3)[31] (see "Methods" section) and determine the fluctuation function $F(s)$, which specifies how the natural fluctuations of the record in time segments of length s scale with s. For long-term persistent data, $F(s) \sim s^h$ where $h > 1/2$ is the Hurst exponent (see "Methods" section). Supplementary Fig. 3a shows $F(s)$ for the Berkeley record between 1850 and 2023 (2088 months). The figure shows that $F(s)$ exhibits a slightly larger Hurst exponent at intermediate scales than at large scales ($h \cong 0.94$). Accordingly, when we consider a shorter subsequence of the record, e.g., the period between 1970 and 2023 (648 months), we do not observe the asymptotic Hurst exponent $h \cong 0.94$, but the intermediate one

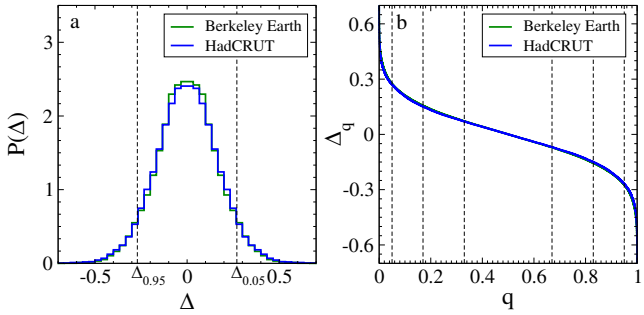

Fig. 2 | Probability density and quantiles of natural trends. a Probability density $P(\Delta)$ and **b** q-quantile Δ_q of the natural trends Δ in the surrogate data for the Berkeley Earth and HadCRUT data sets between 1970 and 2023, as a function of q. With probability q, a trend Δ is above Δ_q. For $q = 0.05$, 0.1, 0.17, 0.33, 0.67, 0.83, 0.9, and 0.95, the quantiles are $\Delta_{0.05} = 0.27$, $\Delta_{0.1} = 0.21$, $\Delta_{0.17} = 0.15$, $\Delta_{0.33} = 0.07$, $\Delta_{0.67} = -0.07$, $\Delta_{0.83} = -0.15$, $\Delta_{0.9} = -0.21$, and $\Delta_{0.95} = -0.27$.

$h \cong 1.05$ (see Supplementary Fig. 3b). We discuss in Supplementary Note 3 that the crossover behavior in F is caused by the El Niño Southern Oscillation (ENSO).

(ii) Next we use the method of Lennartz and Bunde[23] (for more details, see ref. 24 and the "Methods" section) to generate a large number of surrogate time series of length 2088 with a Hurst exponent $h = 0.94$ (see "Methods" section). We consider in each record the last 648 data points and normalize them such that their standard deviation is identical to the standard deviation $\sigma = 0.149$ of the Berkeley Earth data set around the trend line between 1970 and 2023. The resulting records can serve as a set of surrogates for the monthly Berkeley data between 1970 and 2033 when the role of ENSO is being disregarded. For the HadCRUT record, we proceeded analogously. We will refer to this data set as Set I.

(iii) To take into account the effect of ENSO, we consider in Set I only those records where the last 648 data points are characterized by a DFA3 Hurst exponent h close (±0.01) to 1.05. This way, we obtained $N = 38{,}000$ surrogate records for the Berkeley record between 1970 and 2023. For the HadCRUT record where the Hurst exponents are $h = 0.93$ (1850–2023) and 1.11 (1970–2023), we proceeded analogously. We refer to this data set as Set II.

We show in Supplementary Table 1 that our natural variability-focused assessment of the climate overshooting timing depends only very slightly on the choice of the surrogate data set. In the following, we will therefore limit ourselves to Set II, and by surrogate data, we will therefore always understand Set II.

To estimate the q-quantile Δ_q we performed, in each of the N data sets of length $L = 648$, a linear regression (as shown in Fig. 1): from the regression line $r_i = bi + d$, $i = 1, 2 \cdots, L$, we obtain the magnitude of the trend $\Delta = b(L-1)$. We number the N Δ-values according to their rank, $\Delta^{(1)} < \Delta^{(2)} < \cdots < \Delta^{(n)} < \Delta^{(n+1)} < \cdots < \Delta^{(N-1)} < \Delta^{(N)}$. Above $\Delta^{(n)}$, there are $(N-n)$ Δ-values. Accordingly, Δ-values above $\Delta^{(n)}$ occur with probability $q = (N-n)/N$. Thus the desired q-quantile of the natural trends is simply $\Delta_q = \Delta^{(N(1-q))}$.

Figure 2 shows the probability density $P(\Delta)$ and Δ_q for both the Berkeley Earth data and the HadCRUT record in the linear trend regime between 1970 and 2023. The Figure shows that in both records, the Δ_q-values are practically identical, i.e., despite the different ways both records have been obtained and despite the different offsets Δ_{off} in their absolute temperature value, both datasets exhibit the same underlying natural variability. The values of the quantiles for $q = 0.05$, 0.1, 0.17, 0.33, 0.66, 0.83, 0.9, and 0.95 are listed in the Figure Caption.

Assessment of future global warming and the time remaining until the 1.5 °C and 2.0 °C thresholds are exceeded

Figure 3 shows the conceptual setup of our method (here based on the surrogates of the Berkeley Earth data): (a) displays 2 records of the surrogate data, with (natural) trends identical to the 0.05 quantile $\Delta_{0.05} = 0.27$ °C (upper curve) and the 0.95 quantile $\Delta_{0.95} = -\Delta_{0.05}$ (lower curve), such that 90% of the natural trends are between both trend lines. For simplicity, the lower curve is a mirror image of the upper one. A not-yet-applied forcing trend is shown as a red line. (b) When we superimpose the anthropogenic trend (red line) and the natural fluctuations, we obtain 2 surrogates for the observed global mean temperature trend (upper and lower blue lines). The observed trend line can be equally likely below or above the anthropogenic trend line.

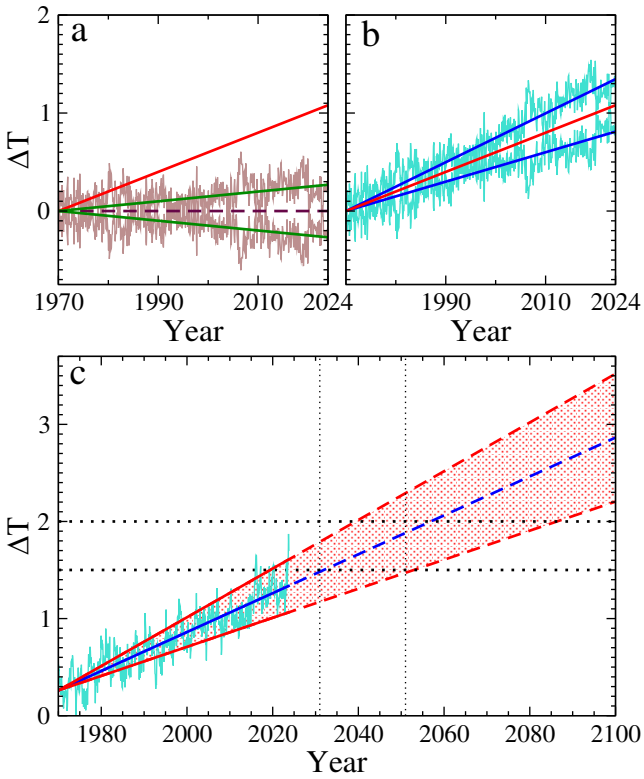

Fig. 3 | Observed trend, natural trends, and related anthropogenic trends. a Two surrogate records with trends identical to the 0.05 quantile $\Delta_{0.05} = 0.27$ and the 0.95 quantile, $\Delta_{0.95} = -\Delta_{0.05}$. In addition, a not-yet-applied external (anthropogenic) forcing trend is shown as a red line. **b** When the anthropogenic trend (same red trend line as in (**a**)) is imposed on the natural fluctuations of (**a**), the resulting actually observed warming trend (upper and lower blue lines) may be equally likely higher or lower than the anthropogenic trend. Here, the real anthropogenic trend is known, but not which trend will become the actual observed trend. **c** The central turquoise record shows the observed Berkeley Earth data and corresponds to the turquoise curves in (**b**). The observed warming trend between 1970 and 2023 (blue line) corresponds to one of the blue lines in (**b**), however, here it is not known if, e.g., it is the lower or the upper one. That is, the real unknown anthropogenic trend may be higher or lower (red lines) than the observed trend. The upper and lower red trend lines are obtained by adding to the observational trend the lines for the natural trends obtained from our surrogate data with quantiles $\Delta_{0.05}$ and $\Delta_{0.95} = -\Delta_{0.05}$. Thus the observed trend line (blue) is the most likely (median) anthropogenic trend. By construction, the real (unknown) underlying anthropogenic trend is with 90% probability between the two red lines. The dashed lines are the projections into the future. The intersections of the vertical dotted lines in 2031 and 2051 with the dashed red trend lines show the very likely anthropogenic temperature ranges in these years. The intersections of the dashed red lines with the horizontal dotted lines show the very likely periods of time when the thresholds will be passed.

This feature is quantified in Fig. 3c. The figure shows the Berkeley record between 1970 and 2023 with its observed trend line in blue (from Fig. 1) and two anthropogenic trend lines (in red) obtained from the superposition of the observed trend line (from Fig. 1) and the two natural trend lines from Fig. 3a. In plotting the figure we have assumed that the anthropogenic warming will continue at the present rate (dashed lines), see also next subsection. By construction, it is very likely (90% probability) that the future anthropogenic

trend is between the two dashed red trend lines. Figure 3c shows explicitly that the uncertainty in the estimation of the current natural trend is the origin of the uncertainty in the future anthropogenic trend, which may be equally likely above or below the observed warming trend.

For a specific q-value, between 1970 and 2023 the anthropogenic warming rate per month is

$$b_q = (\Delta^* - \Delta_q)/(L-1). \quad (3)$$

For $q = 0.95$ and 0.05 shown in Fig. 3c, $b_q \cong 0.00125$ resp. 0.00209 °C per month for the Berkeley record, and $b_q \cong 0.00124$ resp. 0.00207 °C per month for the HadCRUT record. For $q = 0.83$ and 0.17 (defining the likely range), $b_q \cong 0.00143$ resp. 0.00191 °C per month for the Berkeley record, and $b_q \cong 0.00142$ resp. 0.00189 °C per month for the HadCRUT record.

At the start of the trend line in January 1970, the temperature increase Δ_{off} compared with the 1850–1900 period is 0.26 °C for the Berkeley record and 0.20 °C for the HadCRUT record. Accordingly, in month m (counting from January 1970, i.e., $m = 1$ refers to January 1970 and $m = 648$ to December 2023), the anthropogenic part of the GMST will be, with probability q, above

$$T_q(m) = \Delta_{off} + (m-1)b_q. \quad (4)$$

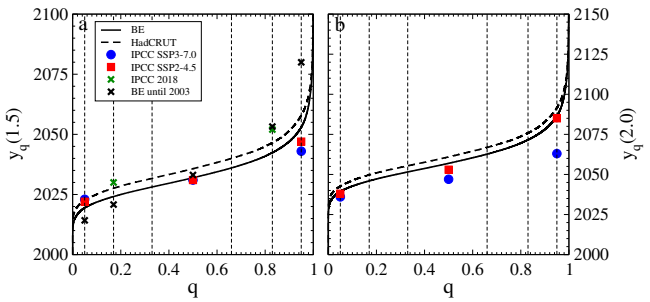

Fig. 4 | Time by which 1.5 °C and 2.0 °C will be exceeded with probability *q*. The figure shows the q-quantiles of the time to exceed **a** the 1.5 °C and **b** the 2.0 °C warming threshold versus q, based on Eqs. (3) and (4). The figure shows in which year y the thresholds will be exceeded, as a function of the probability q, for the Berkeley Earth (BE) and the HadCRUT records, both considered until 2023. The full symbols are the IPCC AR6 estimates for the high emissions scenario SSP3-7.0 and the intermediate emissions scenario SSP2-4.5. The black crosses are based on the Berkeley Earth data until 2003. The green crosses are based on the IPCC 2018 report.

By definition, $T_q(1) = \Delta_{off}$ and $T_{0.5}(648) = \Delta_{off} + \Delta^*$. Equation (4) yields the projected temperature range in month m and allows to determine the likely and very likely period of time when a certain threshold Θ will be passed. Equation (3) reveals that the q-quantiles of the natural trends shown in Fig. 2 are the only relevant quantity here. They are obtained from the observations of the past 54 years (1970–2023) and determine the uncertainties of the anthropogenic trend in both the observations and the projections.

Accordingly, the best estimates and *very likely* ranges (90% probability) of the GMST based on the Berkeley record are 1.48 [1.18 to 1.79] °C in the near term ($m = 733$, January 2031) and 1.88 [1.48–2.29] °C in the mid-term ($m = 873$, January 2051). The respective *likely* ranges (66% probability) are [1.31–1.66] °C (2031) and [1.65–2.12] °C (2051). For estimates based on the HadCRUT record, one has to subtract about 0.07 °C from each temperature value. For completeness, we list also the results near the end of the century. We do not think that our assumption of a constant anthropogenic warming trend will be correct in 2091, but the results can serve as a lower bound, when the warming will be faster, or as an upper bound in the case that the anthropogenic warming rate will be lower than today. For January 2091 ($m = 1453$), the best, very likely and likely ranges for the Berkeley Earth record are 2.68, [2.08–3.29] °C and [2.34–3.03] °C, respectively.

Figure 4 shows the times when the thresholds 1.5 °C and 2.0 °C will be passed, as a function of the probability q. For the 1.5 °C threshold, the best estimates and very likely ranges are 2031 [2019–2052] (Berkeley) and 2035 [2022–2057] (HadCRUT). The likely ranges are: [2024–2042] (Berkeley) and [2027–2046] (HadCRUT). The probability that the 1.5 °C-threshold has already been passed at present (June 2025) is 21.8% for the Berkeley and 10.9% for the HadCRUT record. For the 2.0 °C threshold, the best estimates and very likely ranges are 2056 [2039–2086] (Berkeley) and 2060 [2042–2091] (HadCRUT). For the likely ranges, the estimates are [2046–2071] (Berkeley) and [2049–2075] (HadCRUT).

We would like to note that these results are based on surrogate data Set II, which takes into account the effect of ENSO. Surrogate data Set I yields very similar results, see Supplementary Note 4. This demonstrates that the quasi-periodic influence of ENSO has only a minimal effect on our estimates.

Consistency check

For checking the consistency of our approach, we have regarded the Berkeley Earth data between 1850 and 2003, and used the same approach to assess the range of the anthropogenic warming in 2031 and 2051, as well as the time ranges when the anthropogenic warming will exceed the 1.5 and 2.0 °C thresholds. Table 1 shows that the estimates of the median temperatures and median times based on data until 2003 agree quite well with the estimates based on 20 years more data. The estimates of the *likely*

Table 1 | Comparison of the estimates based on natural variability and IPCC scenarios

	BE until 2003	BE until 2023	SSP2–4.5	SSP3–7.0
Temperature 2031	1.46 °C	1.48 °C	1.5 °C	1.5 °C
Likely range	[1.17–1.75] °C	[1.31–1.66] °C		
Very likely range	[0.95–1.97] °C	[1.18–1.79] °C	[1.2–1.8] °C	[1.2–1.8] °C
Temperature 2051	1.85 °C	1.88 °C	2.0 °C	2.1 °C
Likely range	[1.47–2.23] °C	[1.65–2.12] °C		
Very likely range	[1.18–2.52] °C	[1.48–2.29] °C	[1.6–2.5] °C	[1.7–2.6] °C
1.5 °C threshold	2033	2031	2031	2031
Likely range	2020–2053	2024–2042		
Very likely range	2014–2079	2019–2052	2022–2047	2023–2043
2.0 °C threshold	2058	2056	2053	2047
Likely range	2041–2087	2046–2071		
Very likely range	2032–2124	2039–2086	2038–2085	2036 to 2063

The table compares our estimates based on the Berkeley Earth (BE) data until 2003 and until 2023 with the IPCC SSP2–4.5 and SSP3–7.0 scenarios. It shows the GMST increase in 2031 and 2051, as well as the corresponding likely and very likely ranges, based on Eqs. (3) and (4). The table also compares the estimates for the time when 1.5 °C and 2.0 °C will be exceeded and the corresponding likely and very likely ranges. The IPCC estimates are based on the average of 20 year periods, and we show the midpoint of these periods.

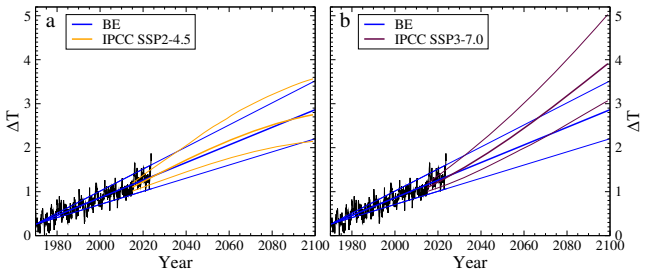

Fig. 5 | Projections based on the Berkeley Earth (BE) record and projections of the IPCC SSP scenarios. a Our median projection based on the BE record (thick blue line) and the corresponding 0.05 and 0.95 lower and upper bounds (thin blue lines), and the median projection for the intermediate emissions scenario SSP2–4.5 (thick orange line) and the corresponding very likely range (0.05–0.95). **b** Same as **a** but for the high emissions scenario SSP3–7.0.

temperature and time ranges made in 2003 are quite close to the estimates of the *very likely* temperature and time ranges made in 2023. This confirms that our approach is internally consistent and actually allowed a quite reasonable projection of future global warming already in 2003.

The fact that our projections based on the shorter data set show a considerably larger uncertainty is a consequence of the long-term persistence in the GMST. In long-term persistent records the slope b of the natural trend decreases with increasing record length L[26]. Since the natural trends are the main source for the uncertainty in the anthropogenic warming trend estimated here, the uncertainty is larger in the shorter data set and smaller in the longer data set. In other words, when more observational data is available in the future, the likely and very likely ranges reported in Table 1 will be reduced.

Comparison with the Earth System Model assessments

In the 6th assessment report (AR6), the IPCC[4] assessed the climate response to 5 illustrative scenarios based on Shared Socioeconomic Pathways (SSPs) that cover the range of possible future development of anthropogenic drivers of climate change found in the literature[32]. Very high and high greenhouse gas (GHG) emissions scenarios (SSP5–8.5 and SSP3–7.0) have CO_2 emissions that roughly double from current levels by 2050 and 2100, respectively. The intermediate GHG scenario (SSP2–4.5) has CO_2 emissions remaining around current levels until 2050. The very low and low GHG emissions scenarios (SSP1–1.9 and SSP1–2.6) have CO_2 emissions declining to net zero around 2050 and 2070, respectively, followed by varying levels of net negative CO_2 emissions. Given the fact that the world's largest economies, including the USA, China, and the European Union, are making strong efforts to reduce emissions, the very high emission scenario does seem improbable, and at present, it is difficult to see whether the conditions of the low and very low emission scenarios can be achieved.

Thus, we compare our assessments for the range of future anthropogenic warming and the remaining time until the 1.5 and 2.0 °C thresholds will be exceeded with those of the scenarios SSP2–4.5 and SSP3–7.0.

We would like to note that, in contrast to the SSP scenarios, which consider separately pathways for the GHGs and the aerosol forcings, we consider effective anthropogenic trends, which include all the anthropogenic forcings. Figure 5 compares our projection based on the Berkeley Earth record with the IPCC projections based on the SSP2–4.5 and SSP3–7.0 scenarios[33,34]. Please note that here the IPCC projections are assessed projections, which were obtained by weighting the CMIP6 model simulations by their skill to reproduce the past warming trend[11–13]. In addition, an updated assessment of equilibrium climate sensitivity[33] has been used. Our projection concurs remarkably well with the SSP2-4.5 scenario regarding the median value and the lower 0.05 and upper 0.95 ranges. In particular, in the near term (20y running average at 2031), the best estimate and very likely ranges are identical in both scenarios[4], 1.5 [1.2–1.8] °C, which fully agrees with our estimate of the anthropogenic warming based on the Berkeley record. In the mid-term (20y running average at 2051), they are nearly identical, 2.0 [1.6–2.5] °C (SSP2–4.5) and 2.1 [1.7–2.6] °C (SSP3–7.0). Again, both estimates are quite close to our estimate of 1.9 [1.5, 2.3] °C based on the Berkeley record. In the long term (2091), both scenarios differ strongly, 2.7 [2.1–3.5] °C (SSP2–4.5) and 3.6 [2.8–4.6] °C (SSP3–7.0). Our estimate 2.7 [2.1–3.3] °C (Berkeley) is quite close to the SSP2–4.5 estimate.

Next, we compare the assessments of the remaining time until the 1.5 and 2.0°C thresholds will be exceeded, see also Fig. 4. Under the high GHG emissions scenario (SSP3–7.0), the central estimate and the very likely range when the midpoint of a 20 year running average will cross 1.5 °C are 2031 and [2023–2043]. Under the intermediate GHG emissions scenario (SSP2–4.5), the corresponding years are 2031 and [2022–2047]. Both estimates and their uncertainties are quite close to our estimates: 2031 [2019–2052] and 2035 [2022–2057] based on the Berkeley Earth and the HadCRUT record, respectively.

For the 2.0 °C threshold, the central estimates and very likely ranges are 2047 [2036–2063] and 2053 [2038–2085] under the SSP3–7.0 and SSP2–4.5 scenarios, respectively. Again, the SSP2–4.5 estimate is close to our estimates 2056 [2039–2086] (Berkeley) and 2060 [2042–2091] (HadCRUT), but based on our analysis, there may be a little more time until the 2.0 °C threshold is exceeded.

It is worth noting that the likely and very likely ranges obtained from our data-driven approach stem from the q-quantile of the anthropogenic trend, which is associated with the impacts of natural variability in the observations from 1970 to 2023. They are different from the uncertainty sources of the ESM projections, but a direct comparison here indicates that our simple data-driven approach based on observations of the past 54 years already has similar skills as the ESMs in projecting future warming trends. When more data is available in the future, we expect further reduced uncertainties based on our approach.

Conclusions

In our data-driven approach for estimating future warming, we used the fact that the observed warming trend is the superposition of the anthropogenic warming trend driven by the anthropogenic forcings and a natural trend driven by the physiogenic variability of the global climate system. To estimate the natural trend, we exploited the long-term persistence property of the planetary surface temperature and generated a large number of surrogate data for the natural variability of (i) the Berkeley, and (ii) the HadCRUT record between 1970 and 2023, where the observed temperature increases approximately linearly in both cases. The surrogate data enabled us to determine the q-quantile of the natural trends as well as the related q-quantile of the anthropogenic trend, between 1970 and 2023.

By assuming that the anthropogenic trend will continue to increase at the current rate, we could estimate the q-quantile of the anthropogenic trend in the coming decades and this way assess the range of warming in the near term (around 2031) and the midterm (around 2051) as well as the range of the years in which the 1.5 °C and the 2.0 °C warming thresholds, which are crucial to avoid tipping processes[35,36], will be likely and very likely exceeded.

Our data-driven statistical approach is complementary to the computationally demanding Earth System Model approach used by the IPCC, where the uncertainty is not only arising from the internal variability, but also related to the ESMs' representation of physical processes of the Earth System. It has been well recognized that the ESMs can respond to external forcings differently. This has been named "model uncertainty", which is non-negligible in future projections of a few decades to even longer time scales, and motivates the IPCC to apply various methods (e.g., the observation-based constraint methods) to reduce it.

In contrast, in our approach, the uncertainty in future anthropogenic warming comes from the fact that the natural trend in the past can only be assessed in a statistical way, i.e., one can only specify the probability that the natural trend is above (or below) a certain value. Since the natural trend and the anthropogenic trend are superimposed, which results in the observed warming trend, the uncertainty in the anthropogenic trend is a direct

consequence of the uncertainty in the natural trend. This uncertainty extends into the future and directly determines the uncertainty in the quantities considered here. We would like to note that our here-discussed linear approach (where we assume that the anthropogenic warming will continue to increase with the same rate as before) can be adapted to the case when the future anthropogenic warming is assumed to increase in a certain non-linear fashion. While considering this case requires a much higher computational cost, the linear approach discussed here can be used as a reasonable first order approximation.

We consider it as remarkable that both our data-driven approach, which is solely based on the observational data of the past, and the Earth System Model approach under the high and intermediate GHG emissions scenarios, yield quite similar projections for the range of warming in the near term and midterm as well as for the range of the years in which the 1.5 °C and the 2.0 °C warming threshold will be likely/very likely exceeded. Since both approaches are methodologically completely independent of each other, given the observational record that both use as a reference, they support each other strongly. Our tentative explanation for this important match is the implicit accounting for natural climate variability in the model ensembles employed by the IPCC and other assessment schemes: Each of the individual complex simulation machines contain many knobs (fits, parametrizations, flux corrections, bias adjustments, etc.) that can be turned to reconcile model outputs with the historical data. However, a deeper exploration of the coincidence we found is certainly required.

In any case, the policy-relevant bottom line of our study is that breaching the 1.5° C-warming threshold seems unavoidable. On the other hand, recent investigations on the so-called "Zero Emissions Commitment" suggest that zero CO_2 emissions likely imply flat future temperatures[37], so there is some hope that breaching the 2 °C-threshold might be averted[38] if global emissions can be eliminated before 2050. Since the latter may either not be feasible or not suffice, overshoot management needs to be considered, i.e., the mid-term return to below-2 °C temperature regimes through negative emissions.

Methods

Data

In this study, we use the Berkeley Earth and HadCRUT5 monthly global mean surface temperature (GMST) data sets that cover the period from January 1850 to December 2023.

Detection of the persistence properties of the GMST data sets

For analyzing the natural persistence structure of both records, we applied the standard Detrended Fluctuation Analysis of order $n = 3$ (DFA3). In DFA3[31], one measures the natural variability of a record of length L by dividing it into L/s non-overlapping segments of length s and studying how the fluctuations in the segments change with the segment length s. To this end, one determines for each data point i, $i = 1, 2, \ldots, s$, in segment v the cumulative sum $Y_v^{(i)}$ of the data and determines the variance $F_v^2(s)$ of $Y_v^{(i)}$ around the best polynomial fit of order $n = 3$, this way eliminating systematically linear and quadratic trends in the original data set. After averaging $F_v^2(s)$ over all segments v and taking the square root, we arrive at the DFA3 fluctuation function $F(s)$. One can show that asymptotically

$$F(s) \sim s^h. \tag{5}$$

The exponent h can be associated with the Hurst exponent. For uncorrelated and short-term correlated data, $h = 1/2$. For h above 1/2, the data are long-term persistent. Long-term persistence occurs in a large number of climate data, among the most prominent examples are temperature[28,39,40], river runoff[21,27,41–44], relative humidity[45,46] and sea-level[47,48] data. The larger h is, the stronger is the long-term persistence in the time series, and the more pronounced is its mountain-valley structure. The detrended fluctuation analysis allows to distinguish between short- and long-term persistent processes[49] and provides reliable results for segment lengths s between 10 and $L/4$[31], and data lengths L above 400 data points. The exponent h can be determined by a power-law fit between 10 and $L/4$.

Generation of long-term persistent surrogate records

For generating the proper ensemble of surrogate data for both GMSTs, with fixed length $L = 2088$ and fixed Hurst exponent h ($h = 0.94$ for the Berkeley record and $h = 0.93$ for the HadCRUT record), we closely follow the method of refs. 23,24,26. The method has been successfully applied to, among others, the analysis of trends in local, regional and global surface air temperatures, sea level rise and sea ice extent[23,25,26,47,49–54] and consists of 2 steps:

In step (i), we employ the Fourier Filtering Technique (FFT) (e.g., refs. 24,55) to generate Gaussian distributed long-term persistent records of length $L_0 = 2^{21}$, with (global) Hurst exponents $h_g = 0.81, 0.82, 0.83, \ldots, 1.19, 1.20$. For each h_g value, we generated 1000 records in the case of Berkeley Earth and due to the larger mismatch between the two Hurst exponents, see below, 10,000 records in the case of HadCRUT.

In step (ii), we extracted, from each record, 1004 non-overlapping subsequences of length 2088 (corresponding to the number of months in the GMST records between 1850 and 2023) and applied DFA3 to each record. Since the Hurst exponents of the subsequences fluctuate around their global value due to finite size effect (see Supplementary Note 5), we took into account only those subsequences where the h-value was between 0.93 and 0.95 for the Berkeley record and between 0.92 and 0.94 for the HadCRUT record. We checked that values from outside the above range of global Hurst exponents do not contribute to our results.

We consider in each record the last 648 data points and normalize them such that their standard deviation is identical to the standard deviation of the respective GMST around the trend line between 1970 and 2023. The resulting records can serve as a set of surrogates for the monthly data of both GMSTs between 1970 and 2023 when the role of ENSO is being disregarded. We will refer to this surrogate data set as Set I.

In an additional step, for taking into account the larger persistence of the GMSTs between 1970 and 2023 due to ENSO, we considered only those surrogate records in Set I that are characterized by a DFA 3 Hurst exponent h close (±0.01) to the observed exponents $h = 1.05$ (Berkeley), $h = 1.11$ (HadCRUT). We refer to these data set as Set II.

This way, we create surrogate data that match the Hurst exponents of the observed GMSTs, while taking fully into account the inherent uncertainty due to finite data length. For a discussion of the sensitivity of the natural trends on the Hurst exponent, see Supplementary Note 6 and ref. 26, and for a discussion of the influence of measurement errors, see Supplementary Note 7.

Data availablility

The Berkeley Earth Global Temperature data is available at: https://berkeleyearth.org/data/. The HadCRUT5 global mean temperature data is available at: https://crudata.uea.ac.uk/cru/data/temperature/. The IPCC SSP2–4.5 and SSP3–7.0 global temperature projections are available at: https://catalog.ceda.ac.uk/uuid/98af2184e13e4b91893ab72f301790db.

Code availablility

The codes used to produce these results are available from the first author on request.

Received: 15 October 2024; Accepted: 27 June 2025;
Published online: 21 July 2025

References

1. Meinshausen, M. et al. Realization of Paris Agreement pledges may limit warming just below 2 °C. *Nature* **604**, 304–309 (2022).
2. Matthews, H. D. & Wynes, S. Current global efforts are insufficient to limit warming to 1.5 °C. *Science* **376**, 1404–1409 (2022).
3. IPCC, Global Warming of 1.5 °C. An IPCC Special Report on the impacts of global warming of 1.5 °C above pre-industrial levels and related global greenhouse gas emission pathways, in the context of

strengthening the global response to the threat of climate change, sustainable development, and efforts to eradicate poverty (eds Masson-Delmotte, V. P. et al.). (Cambridge University Press, 2018).
4. IPCC, Climate Change 2021: The Physical Science Basis. Contribution of Working Group I to the Sixth Assessment Report of the Intergovernmental Panel on Climate Change (Masson-Delmotte, V. P. et al eds.) (Cambridge University Press, 2021).
5. Berkeley Earth, June 2024 Temperature Update. https://berkeleyearth.org/june-2024-temperature-update/.
6. Seneviratne, S. I. et al. The many possible climates from the Paris Agreement's aim of 1.5 °C warming. *Nature* **558**, 41–49 (2018).
7. Betts, R. A. et al. Approaching 1.5 °C: how will we know we've reached this crucial warming mark? *Nature* **624**, 33–35 (2023).
8. Franzke, C. et al. The structure of climate variability across scales. *Rev. Geophys.* **58**, e2019RG000657 (2020).
9. Meehl, G. A. et al. Context for interpreting equilibrium climate sensitivity and transient climate response from the CMIP6 Earth system models. *Sci. Adv.* **6**, eaba1981 (2020).
10. Hausfather, Z., Marvel, K., Schmidt, G. A., Nielsen-Gammon, J. W. & Zelinka, M. Climate simulations: recognize the 'hot model' problem. *Nature* **605**, 26–29 (2022).
11. Liang, Y., Gillett, N. P. & Monahan, A. H. Climate model projections of 21st century global warming constrained using the observed warming trend. *Geophys. Res. Lett.* **47**, e2019GL086757 (2020).
12. Tokarska, K. B. et al. Past warming trend constrains future warming in CMIP6 models. *Sci. Adv.* **6**, 12, eaaz9549 (2020).
13. Ribes, A., Qasmi, S. & Gillett, N. P. Making climate projections conditional on historical observations. *Sci. Adv.* **7**, eabc0671 (2021).
14. Lovejoy, S. Return periods of global climate fluctuations and the pause. *Geophys. Res. Lett.* **41**, 4704–4710 (2014).
15. Watanabe, M. et al. Contribution of natural decadal variability to global warming acceleration and hiatus. *Nat. Clim. Change* **4**, 893–897 (2014).
16. Kay, J. E. et al. The Community Earth System Model (CESM) large ensemble project: a community resource for studying climate change in the presence of internal climate variability. *Bull. Am. Meteorol. Soc.* **96**, 1333–1349 (2015).
17. Lehner, F. et al. Partitioning climate projection uncertainty with multiple large ensembles and CMIP5/6. *Earth Syst. Dyn.* **11**, 491–508 (2020).
18. Maher, N., Power, S. B. & Marotzke, J. More accurate quantification of model-to-model agreement in externally forced climatic responses over the coming century. *Nat. Commun.* **12**, 788 (2021).
19. Deser, C. et al. Effects of macro vs. micro initialization and ocean initial-condition memory on the evolution of ensemble spread in the CESM2 large ensemble. *Clim. Dyn.* **63**, 62 (2025).
20. Merrifield, A. L., Brunner, L., Lorenz, R., Medhaug, I. & Knutti, R. An investigation of weighting schemes suitable for incorporating large ensembles into multi-model ensembles. *Earth Syst. Dyn.* **11**, 807–834 (2020).
21. Mandelbrot, B. B. *Gaussian Self-Affinity and Fractals* (Springer, New York, Berlin, Heidelberg, 2001).
22. Rybski, D., Bunde, A., Havlin, S. & von Storch, H. Long-term persistence in climate and the detection problem. *Geophys. Res. Lett.* **33**, L06718 (2008).
23. Lennartz, S. & Bunde, A. Trend evaluation in records with long-term memory: application to global warming. *Geophys. Res. Lett.* **36**, L16706 (2009).
24. Lennartz, S. & Bunde, A. Distribution of natural trends in long-term correlated records: a scaling approach. *Phys. Rev. E.* **84**, 021129 (2011).
25. Bunde, A., Ludescher, L., Franzke, C. & Büntgen, U. How significant is West Antarctic warming? *Nat. Geosci.* **7**, 246 (2014).
26. Tamazian, A., Ludescher, J. & Bunde, A. Significance of trends in long-term correlated records. *Phys. Rev. E.* **91**, 032806 (2015).
27. Hurst, H. E. Long-term storage capacity of reservoirs. *Trans. Am. Soc. Civ. Eng.* **116**, 770 (1951).
28. Blesić, S., Zanchettin, D. & Rubino, A. Heterogeneity of scaling of the observed global temperature data. *J. Clim.* **32**, 349–367 (2019).
29. Rohde, R. A. & Hausfather, Z. The Berkeley Earth Land/Ocean temperature record. *Earth Syst. Sci. Data* **12**, 3469–3479 (2020).
30. Morice, C. P. et al. An updated assessment of near-surface temperature change from 1850: the HadCRUT5 Data Set. *J. Geophys. Res.* **126**, e2019JD032361 (2021).
31. Kantelhardt, J. W., Koscielny-Bunde, E., Rego, H. H. A., Havlin, S. & Bunde, A. Detecting long-range correlations with detrended fluctuation analysis. *Phys. A* **295**, 441–454 (2001).
32. O'Neill, B. C. et al. The Scenario Model Intercomparison Project (ScenarioMIP) for CMIP6. *Geosci. Model Dev.* **9**, 3461–3482 (2016).
33. IPCC, Summary for Policymakers. In: Climate Change 2021: The Physical Science Basis. Contribution of Working Group I to the Sixth Assessment Report of the Intergovernmental Panel on Climate Change (eds Masson-Delmotte, V., P. Zhai, A. Pirani, S.L. Connors, C. Péan, S. Berger, N. Caud, Y. Chen, L. Goldfarb, M.I. Gomis, M. Huang, K. Leitzell, E. Lonnoy, J.B.R. Matthews, T.K. Maycock, T. Waterfield, O. Yelekçi, R. Yu, and B. Zhou) pp 3–32 (Cambridge University Press, 2021) https://doi.org/10.1017/9781009157896.001.
34. Fyfe, J., Fox-Kemper, B. & Kopp, R., Garner, G. Summary for Policymakers of the Working Group I Contribution to the IPCC Sixth Assessment Report—data for Figure SPM.8 (v20210809) (2021). NERC EDS Centre for Environmental Data Analysis. https://doi.org/10.5285/98af2184e13e4b91893ab72f301790db.
35. Lenton, T. M. et al. Tipping elements in the Earth's climate system. *Proc. Natl Acad. Sci. USA* **105**, 6, 1786-1793 (2008).
36. Möller, T. et al. Achieving net zero greenhouse gas emissions critical to limit climate tipping risks. *Nat. Commun.* **15**, 1, 6192 (2024).
37. MacDougall, A. H. et al. Is there warming in the pipeline? A multi-model analysis of the Zero Emissions Commitment from CO2. *Biogeosciences* **17**, 2987–3016 (2020).
38. Höhne, N. et al. Wave of net zero emission targets opens window to meeting the Paris Agreement. *Nat. Clim. Change* **11**, 820–822 (2021).
39. Bloomfield, P. & Nychka, D. Climate spectra and detecting climate change. *Clim. Change* **21**, 275 (1992).
40. Koscielny-Bunde, E., Bunde, A., Havlin, S., Roman, H. E., Goldreich, Y. & Schellnhuber, H. J. Indication of a Universal Persistence Law Governing Atmospheric Variability. *Phys. Rev. Lett.* **81**, 729 (1998).
41. Montanari, A., Rosso, R. & Taqqu, M. S. A seasonal fractional ARIMA model applied to the Nile River monthly flows at Aswan. *Water Resour. Res.* **36**, 5, 1249 (2000).
42. Koutsoyiannis, D. Climate change, the Hurst phenomenon, and hydrological statistics. *Hydrol. Sci. J.* **48**, 3–24 (2003).
43. Koscielny-Bunde, E., Kantelhardt, J. W., Braun, P., Bunde, A. & Havlin, S. Long-term persistence and multifractality of river runoff records: detrended fluctuation studies. *J. Hydrol.* **322**, 120 (2006).
44. Tyralis, H. & Koutsoyiannis, D. A Bayesian statistical model for deriving the predictive distribution of hydroclimatic variables. *Clim. Dyn.* **42**, 2867–2883 (2014).
45. Vattay, G. & Harnos, A. Scaling behavior in daily air humidity fluctuations. *Phys. Rev. Lett.* **73**, 768 (1994).
46. Lin, G., Chen, X. & Fu, Z. Temporal-spatial diversities of long-range correlation for relative humidity over China. *Physica A* **383**, 585–594 (2007).
47. Becker, M., Karpytchev, M. & Lennartz-Sassinek, S. Long-term sea level trends: natural or anthropogenic? *Geophys. Res. Lett.* **41**, 15, 5571 (2014).
48. Dangendorf, S. et al. Detecting anthropogenic footprints in sea level rise. *Nat. Commun.* **6**, 7849 (2015).
49. Ludescher, J., Bunde, A., Franzke, C. L. & Schellnhuber, H. J. Long-term persistence enhances uncertainty about anthropogenic warming of Antarctica. *Clim. Dyn.* **46**, 263–271 (2016).

50. Ludescher, J., Bunde, A. & Schellnhuber, H. J. Statistical significance of seasonal warming/cooling trends. *Proc. Natl Acad. Sci. USA* **114**, E2998–E3003 (2017).
51. Yuan, N., Ding, M., Ludescher, J. & Bunde, A. Increase of the Antarctic sea ice extent is highly significant only in the Ross Sea. *Sci. Rep.* **7**, 41096 (2017).
52. Ludescher, J., Yuan, N. & Bunde, A. Detecting the statistical significance of the trends in the Antarctic sea ice extent: an indication for a turning point. *Clim. Dyn.* **53**, 237–244 (2019).
53. Wang, Y., Yan, P., Feng, T., Ji, F., Tang, S. & Feng, G. Detection of anthropogenically driven trends in Arctic amplification. *Clim. Change* **169**, 1–17 (2021).
54. Wang, Y., Yan, P., Ji, F., Huang, B., Fan, P. & Feng, G. Anthropogenic contribution to the rapid warming over the Tibetan Plateau. *Clim. Dyn.* **61**, 329–339 (2023).
55. Turcotte, D. L. *Fractals and Chaos in Geology and Geophysics: Second Edition* (Cambridge University Press, Cambridge, 2010).

Acknowledgements

J. L. was supported by the "Brazil East Africa Peru India Climate Capacities (B-EPICC)" project, which is part of the International Climate Initiative (IKI) of the German Federal Ministry for Economic Affairs and Climate Action (BMWK) and implemented by the Federal Foreign Office (AA). J. L. is also part of the Planetary Boundaries Science Lab's research effort at PIK. N. Y. was supported by the National Natural Science Foundation of China (No. 42475057 and No. 42175068) and the Guangdong Basic and Applied Basic Research Foundation (2023B1515020084).

Author contributions

J.L. led the data analysis, contributed to the interpretation of the results and the revisions of the first draft. N.Y. contributed to the data analysis, the interpretation of the results and the revisions of the first draft. H.J.S. contributed to the interpretation of the results and the revisions of the first draft. A.B. conceived the project, wrote the first draft, contributed to the interpretation of the results and the revisions of the first draft.

Funding

Open Access funding enabled and organized by Projekt DEAL.

Competing interests

The authors declare no competing interests.

Additional information

Supplementary information The online version contains supplementary material available at https://doi.org/10.1038/s43247-025-02525-5.

Correspondence and requests for materials should be addressed to Josef Ludescher or Naiming Yuan.

Peer review information *Communications Earth and Environment* thanks Suzana Blesic and the other, anonymous, reviewer(s) for their contribution to the peer review of this work. Primary Handling Editors: Min-Hui Lo and Alireza Bahadori. A peer review file is available.